Hindawi
Geofluids
Volume 2022, Article ID 8991574, 12 pages
https://doi.org/10.1155/2022/8991574

Research Article

Roof Bolting Anchoring Performance Research on the Entry under the Gob of Close-Distance Coal Seam

Yongjie Yang[1], **Gang Huang**[1] **and Haiyu Ji**[2]

[1]*State Key Laboratory of Mining Disaster Prevention and Control Co-Founded by Shandong Province and the Ministry of Science and Technology, Shandong University of Science and Technology, Qingdao 266590, China*
[2]*Changsha Digital Mine Info Tech CO., LTD, Changsha 410000, China*

Correspondence should be addressed to Gang Huang; huanggang@sdust.edu.cn

Received 14 February 2022; Accepted 12 April 2022; Published 2 May 2022

Academic Editor: Mingwei Chen

Seam spacing plays a crucial role in selecting roof bolting of the close-distance coal seam. This work utilized three methods to determine the minimum roof bolting seam spacing of the lower coal seam (LCS) entry after the upper coal seam (UCS) mining. Based on the entry of the No.3-2 coal seam (LCS) in Chaili Coal Mine in China, theoretical analysis, pull-out bolt test, and numerical simulation were performed to calculate the maximum floor failure depth of the UCS and to determine the minimum seam spacing of the roof bolting. The maximum floor failure depth of the UCS determined through theoretical analysis and numerical simulation is 3.2 m and 3.3 m, respectively. In general, the anchorage length of rock bolting is less than 2.4 m, so the minimum seam spacing is 5.6 m or 5.7 m. To further determine the anchorage performance of the roof, the pull-out test was employed on the entry roof of the LCS. When the seam spacing is no less than 6 m, the test results show that the pull-out force of the bolt is more significant than 30kN; in addition, the numerical simulation results indicate that the roof-to-floor and rib-to-rib convergence are relatively small. Therefore, the LCS entry's minimum roof bolting seam spacing can be determined as 6 m. This study could be used to select and design roof bolting under similar close-distance coal seam conditions.

1. Introduction

The close-distance coal seam (CDCS) reserves are abundant in China [1]. Affected by mining and geological conditions, the mining method of the CDCS is primarily based on experience. Descending mining, which is widely used in the CDCS, first retreats the upper coal seam (UCS) and then develops the entry in the lower coal seam (LCS) until the overburden is stable. The entry in the LCS is mostly located under the gob or chain pillar. Due to the small seam spacing, the mining activity in the LCS will contribute to the destruction of the overburden time after time, which challenges the surrounding rock control of the entry. Therefore, seam spacing is a crucial factor in the entry's support design, especially under the gob in the LCS. Due to the UCS's mining, the LCS roof is badly damaged when the seam spacing is minimal, and the rock bolts anchor in the loose and broken surrounding rock, leading to poor roof anchoring performance. In addition, it is hard to obtain a good support effect with rock bolting. At this time, passive support such as steel arch support is supposed to be taken into account to ensure the surrounding rock stability of the LCS entry. Conversely, when the seam spacing is large, the roof of the LCS seam is relatively complete, and the rock bolt can be anchored in the stable surrounding rock. At this time, the rock bolting could reach well technical and economic effects.

The fracture and development law of the overburden of UCS in CDCS has received a great deal of research attention. Li et al. obtained the development characteristics of the overburden using the geological penetration radar [2, 3]. With a physical similarity simulation (PSS), Li et al. [4] determined the first and the periodic weighting interval of the main roof. Cui et al. [5, 6] used 3DEC to analyze the development law of the overlying strata's cracks in western China. Ning et al. [7] evaluated the height of fractured zones of the CDCS. Zhang et al. [8] researched the overburden's bearing structure and stability characteristics employing numerical simulation, PSS, and theoretical analyses.

Figure 1: The position of Chaili Coal Mine.

Several recent studies have focused on floor failure depth and stress distribution during UCS mining. Zhang et al. [9] built a floor failure mechanical model of the UCS. Sun et al. [10] proposed a mechanical model based on half-plane theory to obtain the evolution law of the floor. Tan et al. [11] utilized micro seismic techniques, numerical simulations, and borehole inspection to explore the distributions of strata failure. By using UDEC, Liu et al. [12] analyzed the stress distribution of LCS.

Recent studies have explored the LCS entry's optimal layout and surrounding rock stability control in CDCS. Wang et al. [13] suggested that the creep characteristics of surrounding rock are the most critical factor in selecting for the entry's layout of the LCS in deep mines. Wu et al. [14] built a mechanical model to research the stress distribution under chain pillars and adopted numerical simulation to select the optimal entry layout in ultra-close coal seams. Xu et al. [15] focused on the different excavation schemes in the CDCS mining and determined to leave a small coal pillar for excavation. Zhang et al. [16] established a layout of the entry using numerical simulation to minimize the risk of disasters. Zhang et al. [17] put forward the grouting reinforcement method of local fractured zones under a super thick hard roof in an ultra-close-distance coal seam. Zhang et al. [18] focused on surrounding rock stability control and technical parameter design for the gob-side entry retained under the gob.

In conclusion, a large body of literature has focused on the fracture and development law of the overburden of UCS, floor failure depth and stress distribution during UCS mining, and the optimal layout and the surrounding rock stability control of LCS entry in CDCS. As the decisive factor of surrounding rock stability control of the LCS entry, it is necessary to deepen the research on seam spacing further. Due to the complexity of mining and geological conditions, rock bolting or steel arch support is widely used in LCS entry. However, quantitative research on roof bolting technology and support parameters according to the seam spacing size has not yet been conducted. In this paper, taking the tailgate of the No.3-2 coal seam (LCS) in Chaili Coal Mine as an example, the performance of roof bolting is comprehensively studied by three methods. First, the theoretical analysis was used to calculate the maximum floor failure depth. Then, the pull-out test was carried out to determine the minimal seam spacing for roof bolting. With the thought that the distribution depth of yield zone of the floor can represent the maximum floor failure depth, the numerical model was established by FLAC3D. In addition, because the rock bolts are supposed to anchor in relatively intact rock mass, the bolts should not reach the edge of the yield zone in the numerical simulation while determining the minimal seam spacing. This study could be used to select and design roof bolting under similar CDCS conditions.

2. Mining and Geological Conditions

Chaili Coal Mine is located in Tengzhou City, Shandong Province, China, as shown in Figure 1. The current mining seam is the No.3 coal seam. No.3 coal seam is divided into No.3-1 coal seam and No.3-2 coal seam, and the thickness of these two coal seams is 4.8 m and 3.2 m, respectively. The seam spacing between No.3-1 coal seam and No.3-2 coal seam varies from 2 m to 9 m. Figure 2 shows the generalized stratigraphy column.

The panel layout for the No.3 coal seam is 150 m wide by 1766 m long, with a 5 m wide chain pillar between the panels. The tailgate in No.3-2 coal seam under the gob is developed with the dimension of 4 m long ×3.2 m wide,

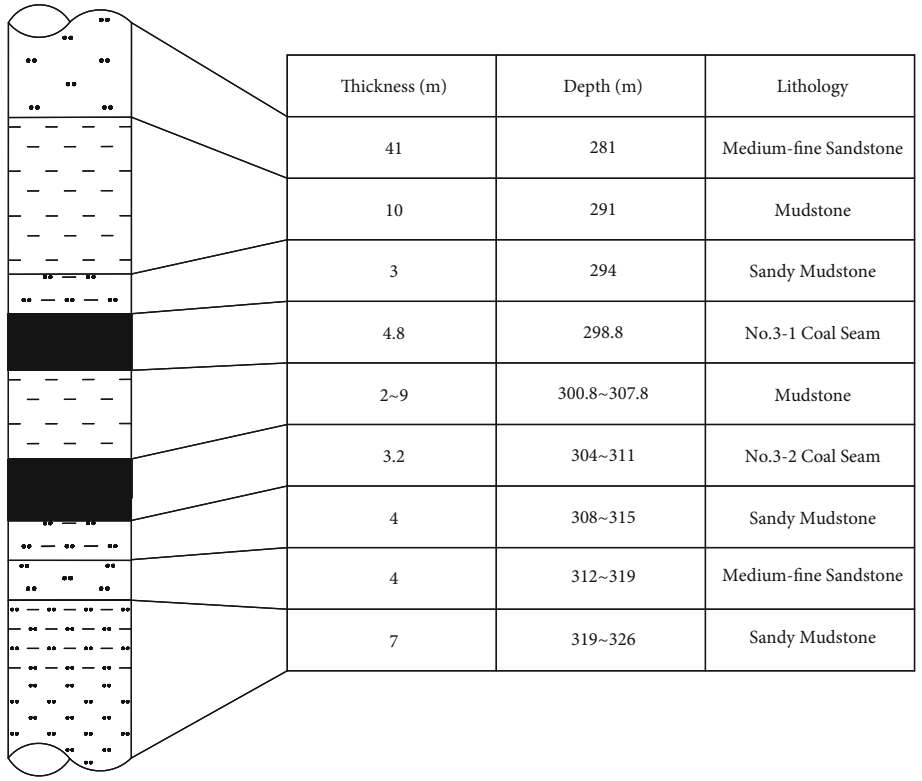

Thickness (m)	Depth (m)	Lithology
41	281	Medium-fine Sandstone
10	291	Mudstone
3	294	Sandy Mudstone
4.8	298.8	No.3-1 Coal Seam
2~9	300.8~307.8	Mudstone
3.2	304~311	No.3-2 Coal Seam
4	308~315	Sandy Mudstone
4	312~319	Medium-fine Sandstone
7	319~326	Sandy Mudstone

Figure 2: Generalized stratigraphy column.

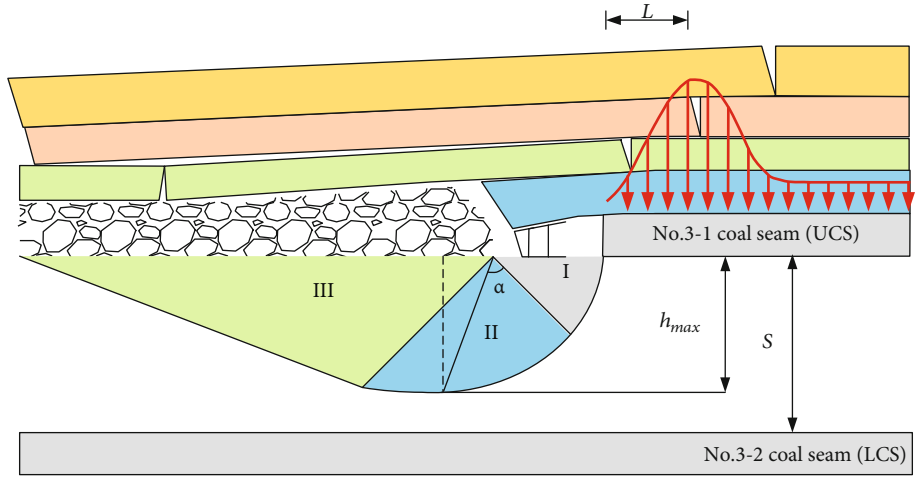

Figure 3: Schematic diagram of the failure depth of No.3-1 coal seam floor.

located directly below the tailgate of No.3-1 coal seam. Furthermore, the cross-section of the tailgate is supported by steel arches.

3. Calculation of the Floor Failure Depth of No.3-1 Coal Seam

According to Zhang [9], the floor failure mechanical model of No.3-1 coal seam (UCS) can be established as shown in Figure 3. Plastic deformation of the floor of the UCS is forming (Area I) when reaching the limit of elasticity. Up to the peak value, the plastic failure zones within the abutment pressure range are linked together, leading to the floor heave of the gob and the plastic deformation transferring from Area II to Area III, forming a continuous sliding surface. At this time, the maximum floor failure depth h_{max} is reached.

Where S is the seam spacing between No.3-1 coal seam and No.3-2 coal seam ranging from 2 m to 9 m.

h_{max} is the maximum floor failure depth of No.3-1 coal seam.

L is the distance between the peak front abutment pressure and the panel.

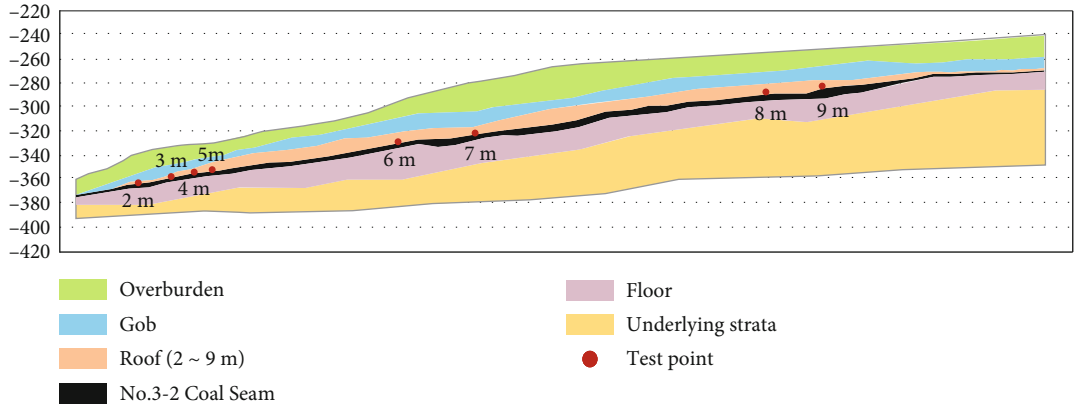

Figure 4: Arrangement of measuring points for bolt pull-out test.

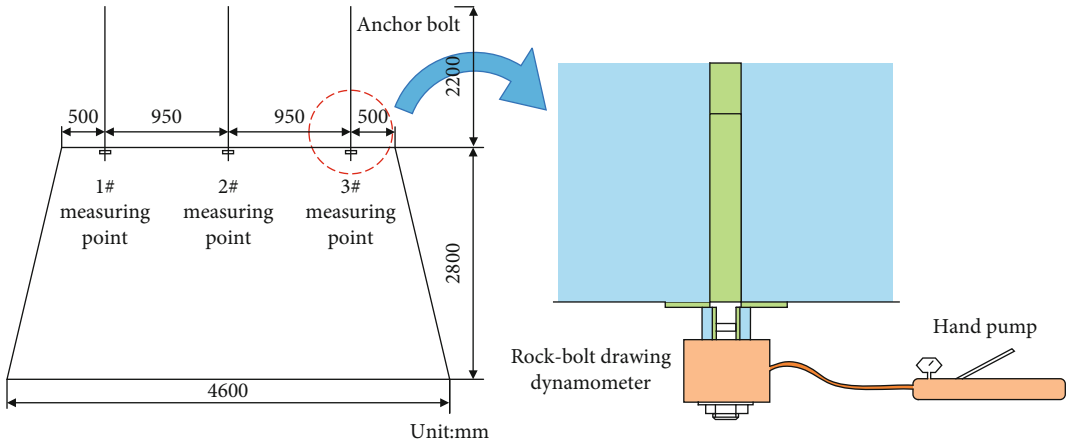

Figure 5: Installation position of test rock bolt of the entry.

Based on the research of Zhang [9] and Sun [19], the floor failure depth can be calculated by Equations (1)–(4):

$$h_{\max} = L \cdot e^{\alpha \tan \varphi_f} \cdot \sin \theta, \tag{1}$$

$$L = \frac{M}{2\zeta f} \ln \frac{K\gamma H + c \cdot \cot \varphi}{\zeta \cdot c \cdot \cot \varphi}, \tag{2}$$

$$\alpha = \varphi_f - \frac{\varphi}{2} + \frac{\pi}{4}, \tag{3}$$

$$\theta = \frac{\varphi_f}{2} + \frac{\pi}{4}, \tag{4}$$

where φ_f is the internal friction angle of the floor, 30°.

φ is the internal friction angle of the No.3-1 coal seam, 28°.

M is the height of the gob, 10.6 m.

K is the stress concentration coefficient, 1.4.

γ is the average bulk density of the overburden, 25 kN/m^3.

H is the average buried depth of the No.3-1 coal seam, 300 m.

c is the cohesion of the No.3-1 coal seam, 1.45 MPa.

f is the friction coefficient of the interface between the No.3-1 coal seam and the floor ($f = \tan \varphi$).

ζ is the triaxial stress coefficient, $\zeta = (1 + \sin \varphi)/(1 - \sin \varphi)$.

Therefore, the maximum floor failure depth of No.3-1 coal seam is as follows:

$$h_{\max} = 3.2\text{m}. \tag{5}$$

4. Roof Bolt Pull-Out Test of No.3-2 Coal Seam under the Gob of No.3-1 Coal Seam

To verify the anchorage performance of the roof of the LCS (No.3-2 coal seam) in the CDCS, the bolt pull-out test was carried out on the roof of No.3-2 coal seam to determine the minimum seam spacing of the roof bolting. If the pull-out force of the bolt is more significant than 30kN, it is considered that the roof is in good anchorage condition [20]. Otherwise, it is considered that the roof is not suitable for rock bolting.

4.1. Test Materials

(1) rock-bolt drawing dynamometer (measuring range is 200kN, and resolution is 1.0kN)

(2) jumbolter

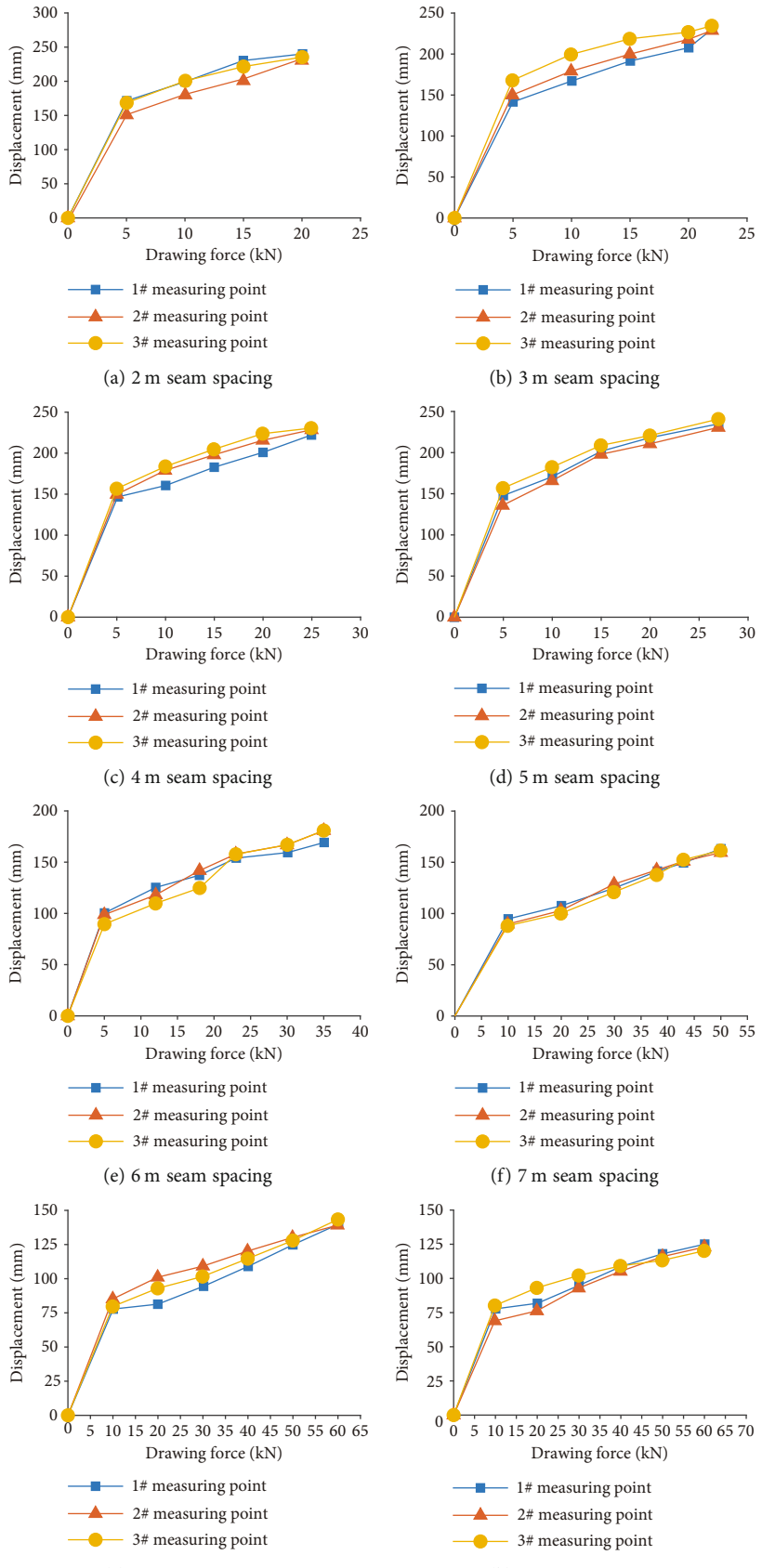

Figure 6: Drawing force-displacement curve of test rock bolt.

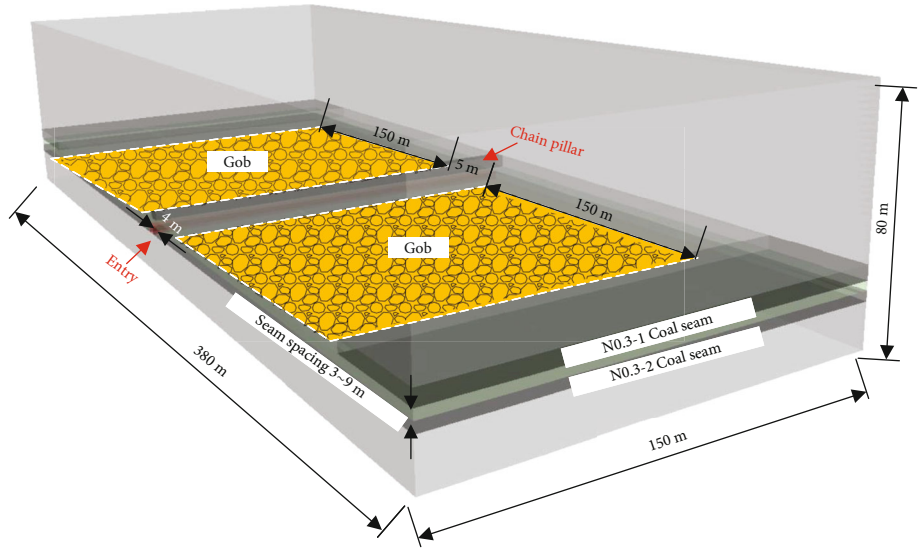

Figure 7: Configuration of the model performed using FLAC3D.

Table 1: Rock strata properties used in the numerical model.

No.	Lithology	Thickness (m)	D (kg/m^3)	K (MPa)	G (MPa)	T (MPa)	c (MPa)	f (deg)
1	Medium-fine sandstone	41	2535	4000	1500	3.00	3.50	35
2	Mudstone	10	2526	2500	1200	6.50	1.38	30
3	Sandy mudstone	3	2731	3340	3280	1.32	1.48	33
4	No.3-1 coal seam	4.8	1462	1500	1020	4.30	1.04	31
5	Mudstone	3-9	2526	2500	1200	6.50	1.38	30
6	No.3-2 mudstone	3.2	1462	1500	1020	4.30	1.04	31
7	Sandy mudstone	4	2738	1800	1100	2.00	2.50	28
8	Medium-fine sandstone	4	2731	6340	9280	4.23	3.48	33
9	Sandy mudstone	7	2731	3340	3280	1.32	1.48	33

Where D is the average density of the rock strata, kg/m^3. K is the bulk modulus of the rock strata, MPa. G is the shear modulus of the rock strata, MPa. T is the tensile strength of the rock strata, MPa. c is the cohesion of the rock strata, MPa. f is the friction angle of the rock strata, deg.

(3) rock bolt (Φ20mm × L2000mm), and resin cartridge (Φ18mm × L600mm)

4.2. Test Method. The test site is shown in Figure 4. Eight test points were arranged at a seam spacing of 2-9 m. The jumbolter was used for the roof bolt installation within two days of headgate excavation, and the bolt pull-out test was carried out within 4 hours.

As shown in Figure 5, three test rock bolts were installed on the entry roof at every test point, the side bolts were 500 mm away from the entry's rib, and the other was in the middle. During bolt installation, the bearing plate must be in close contact with the surface of the surrounding rock of the entry and the installation torque of tension nut was supposed to be relatively large (100~185 Nm) [20, 21]. Therefore, the installation torque of the tension nut was made 150 Nm. The drawing dynamometer should be coaxial with the bolt axis. Meanwhile, ensure that the bolt body does not contact the borehole wall. After installing the test bolt, apply bolt load slowly and continuously, and record bolt displacement every 5kN. Stop the pressure application and record the value of the hand pump until the test bolt fails.

4.3. Test Results and Analysis. Figure 6 indicates that with the increase of drawing force, the displacement of test bolts gradually increases under different seam spacing.

(1) As shown in Figure 6(a), when the initial drawing force reaches 5kN, the displacement of test bolts reaches 170 mm. With the increase of drawing force, the test displacement increases, and the displacement is 250 mm when the drawing force is 20kN. When the drawing force is 21kN (<30kN), all three test bolts fail, indicating that the roof bolt does not have anchor performance under the 2 m seam spacing

(2) Figures 6(b), 6(c), and 6(d) also present that when the drawing force is less than 30kN, all three bolts are pulled out at a seam spacing of 3-5 m

(3) At the 6 m seam spacing, what is striking in Figure 6(e) is that when the drawing force reaches

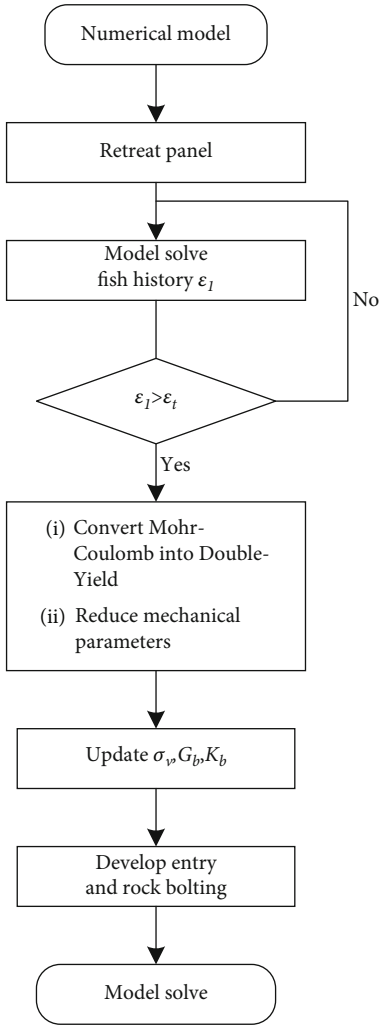

Figure 8: Numerical simulation process by FLAC3D.

30kN, the entire test bolts do not fail. Meanwhile, the displacement of the bolts is small

(4) Figures 6(f), 6(g), and 6(h) show the test results at a seam spacing of 7-9 m. When the drawing force reaches 30kN, the displacement is also small. The maximum drawing force that test bolts fail is 50kN, 60kN, and 65kN, respectively

Consequently, when the seam spacing between No.3-1 coal seam and No.3-2 coal seam is no less than 6 m, the drawing force of test bolts can reach 30kN, the roof of the entry in No.3-2 coal seam is in good anchoring condition.

5. Numerical Modeling

The floor failure depth of No.3-1 coal seam (UCS) and seam spacing significantly influence the coal entry support in the No.3-2 coal seam (LCS). According to the calculation results of the floor failure depth of No.3-1 coal seam in Section 3 and the test results in Section 4, determining the minimum seam spacing of the rock bolts may cause

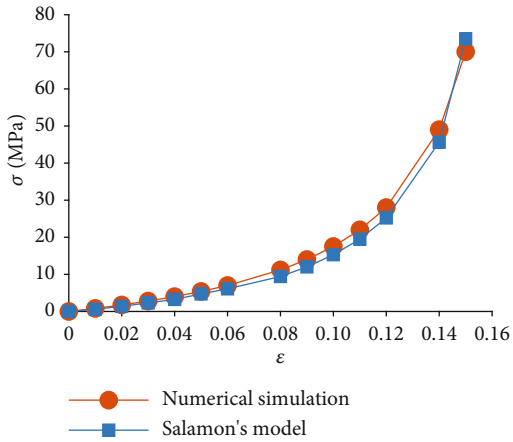

Figure 9: The stress-strain fitting curve.

safety problems. As an effective tool for studying rock mechanics behaviors in underground spaces [22, 23], this section further studies the floor failure depth of the No.3-1 coal seam after mining and the bolt anchoring performance under different seam spacing by numerical simulation.

5.1. Numerical Configuration. A numerical model (Figure 7) using FLAC3D software was established to explore the floor failure depth of No.3-2 coal seam (LCS) and the anchoring performance of roof bolting. The dimensions of the model were 380 m(length) ×150 m(width) ×80 m(height). The panel layout for No.3-1 coal seam (UCS) was 150 m wide by 150 m long with a 5 m wide chain pillar between the panels. The tailgate in No.3-2 coal seam under the gob was excavated with the dimension of 4 m long ×3.2 m wide, located directly below the tailgate of No.3-1 coal seam. A vertical load of 6 MPa was applied to the upper boundary to simulate an overburden pressure by assuming the overlying unit weight is 25kN/m^3. The final scaled rock mass properties are listed in Table 1.

5.2. Simulation Plans. Where σ_v is the vertical stress where the overlying strata apply on gangue.

G_b is the shear modulus of the gangue in the gob.

K_b is the bulk modulus of the gangue in the gob.

As shown in Figure 8, the numerical model was solved in this simulation using the following steps:

(1) the retreat of the two panels of No.3-1 coal seam (UCS) after initial balance, respectively

(2) the development of the entry of No.3-2 coal seam (LCS) with seven different seam spacing (3-9 m)

The caved materials are then compacted and consolidated after panel advances far enough in longwall mining [24, 25]. Consequently, the entry of the LCS in CDCS is supposed to develop until the gob is generally consolidated. The constitutive model applied in the caved zone is Double-Yield to simulate this actual situation. In

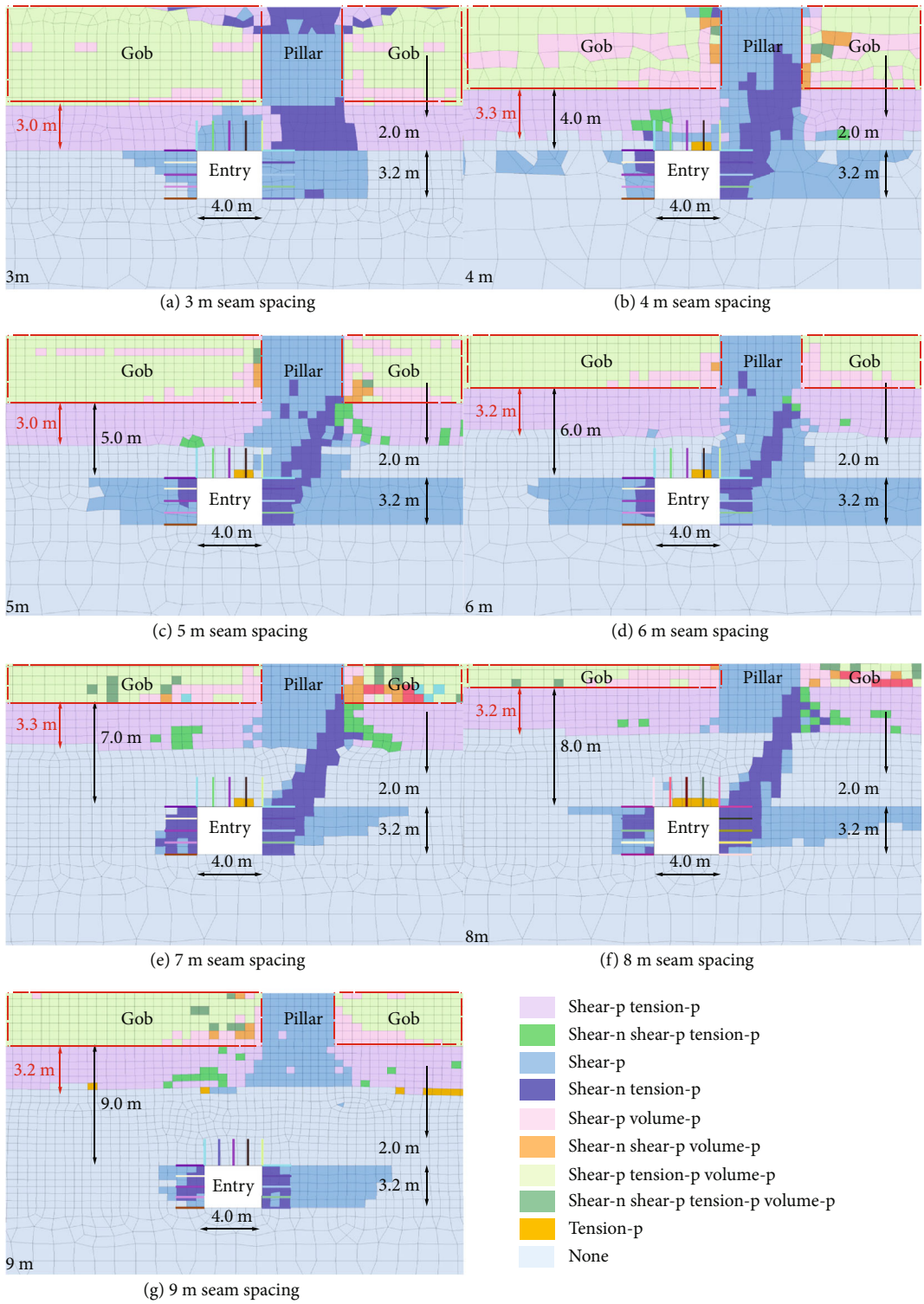

Figure 10: Yield zone distributions around entry for different seam spacing.

addition, the Saint Venant theory is used to determine the range of caved zone, which is given by

$$\varepsilon_1 > \varepsilon_t, \tag{6}$$

where ε_1 is the maximum principal strain.

ε_t is the critical value of tensile strain.

Precisely, the two panels retreated in the No.3-1 coal seam (UCS) after several timesteps. According to Equation (6), when $\varepsilon_1 > \varepsilon_t$, it is considered that the overburden of the UCS has collapsed. Therefore, customize the function in fish to determine the range of caved zone, and compare the results with those calculated by empirical formula, as shown in Figure 9. If the range of caved zone is consistent with the

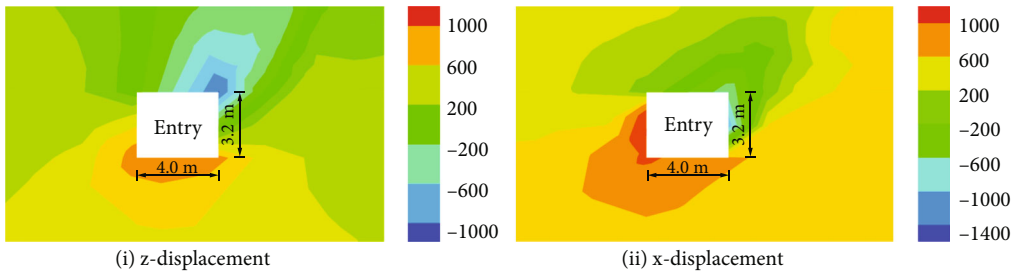

(i) z-displacement (ii) x-displacement

(a) 3 m seam spacing

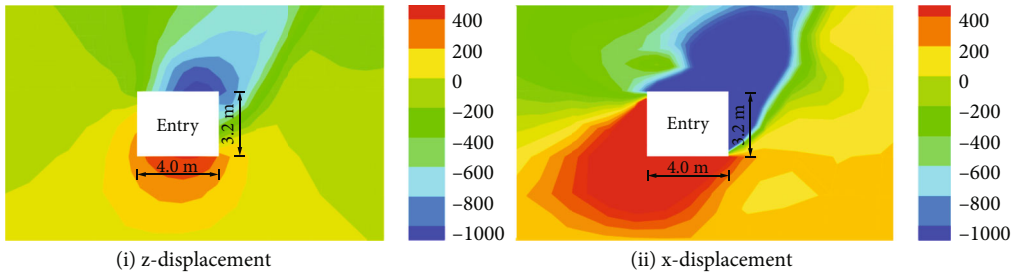

(i) z-displacement (ii) x-displacement

(b) 4 m seam spacing

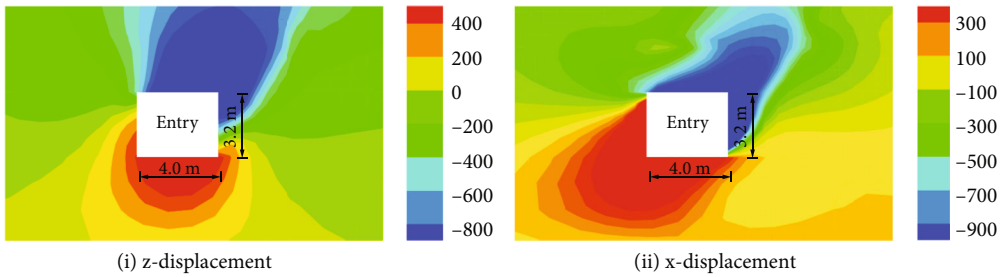

(i) z-displacement (ii) x-displacement

(c) 5 m seam spacing

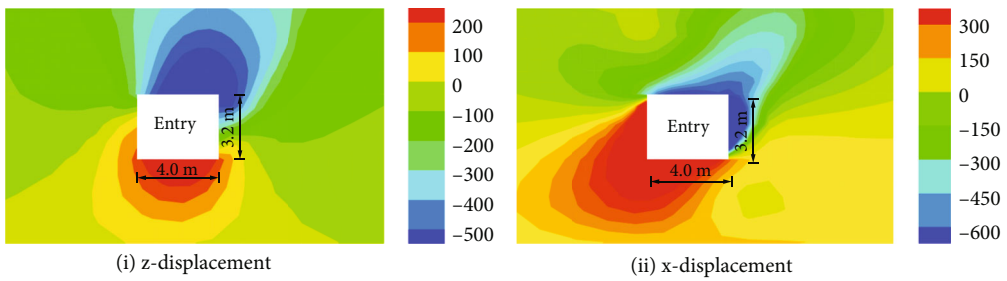

(i) z-displacement (ii) x-displacement

(d) 6 m seam spacing

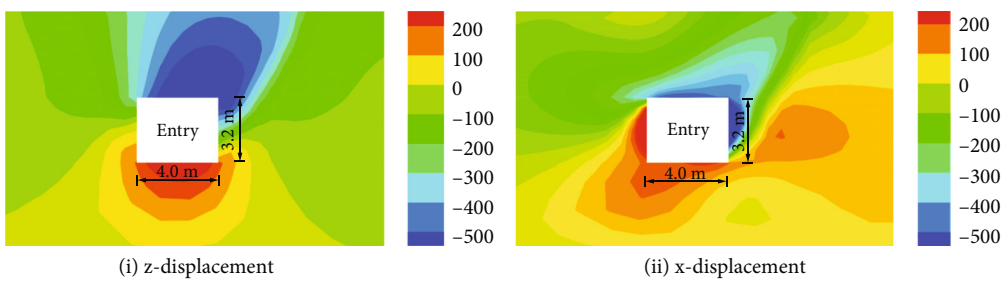

(i) z-displacement (ii) x-displacement

(e) 7 m seam spacing

Figure 11: Continued.

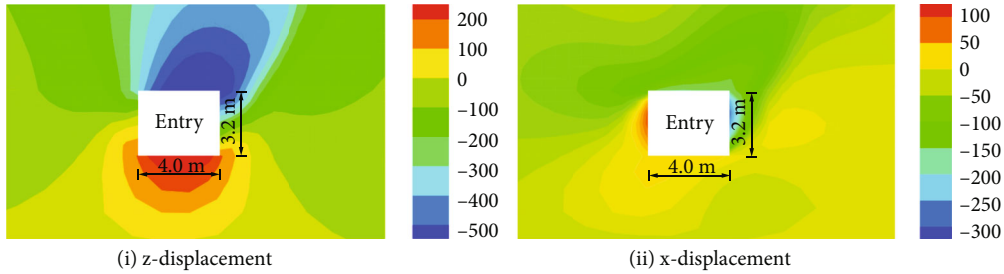

(i) z-displacement (ii) x-displacement

(f) 8 m seam spacing

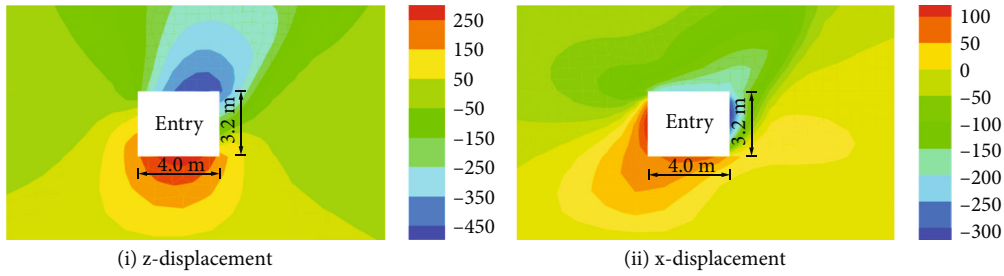

(i) z-displacement (ii) x-displacement

(g) 9 m seam spacing

Figure 11: Displacement distribution around entry for different seam spacing.

result of empirical formula [26], then convert the constitutive model of caved zone from Mohr-Coulomb to Double-Yield. At the same time, the mechanical parameters in the yield zone are reduced to simulate the fractured zone, the vertical stress σ_v, volume modulus K_b, and the shear modulus G_b of the gangue in the gob are updated at regular intervals until the balance is calculated. Based on the research of Bai et al. [27], the properties of double-yield constitutive model can be given by

$$K_b = \frac{4G_b}{3} = \frac{\sigma_v}{2\varepsilon}. \tag{7}$$

As shown in Equation (7), the volume modulus K_b, the shear modulus G_b and the vertical stress σ_v can be expressed as a function of the vertical strain ε. Consequently, after several intervals, such as 50 timesteps, the vertical strain of the gob material is recorded in numerical simulation, and then changes these properties according to Equation (7). Then, the LCS entry is developed once every 5 m and rock bolting until the end of the development.

5.3. Yield Zone Distribution around Entry for Different Seam Spacing. This part is set out to seek the proper seam spacing for roof bolting of the entry of No.3-2 coal seam (LCS). The floor failure depth is reflected by the yield zone of the floor of No.3-1 coal seam (UCS). According to suspension theory, rock bolts are supposed to anchor in relatively intact rock strata. Therefore, the end of the rock bolt had better anchor out of the yield zone. Figure 10 shows the yield zone distribution around entry for different seam spacing (3-9 m).

Figure 10 shows that with the increase of seam spacing, the floor failure depth (ranging from 3.0 to 3.3 m) of No.3-1 coal seam (UCS) has no noticeable change, but the yield zone around the entry, particularly the roof, gradually decreases.

(1) Figures 10(a), 10(b), and 10(c) show the yield zone distribution at a seam spacing of 3-5 m. It can thus be seen, the yield zone around entry is large, and the rock bolt cannot anchor in relatively intact rock strata

(2) At the 6 m seam spacing, what stands out in Figure 10(d) is that the end of the rock bolt exactly anchors out of the yield zone. Meanwhile, the distribution of yield zone around entry is small

(3) Figures 10(e), 10(f), and 10(g) also present the distribution of yield zone around entry is not large, and the rock bolt can anchor in the relatively intact rock strata

(4) Thus, when the seam spacing between No.3-1 coal seam and No.3-2 coal seam is no less than 6 m, the distribution of yield zone is not large, and the rock bolt can anchor in relatively intact rock strata

5.4. Deformation of Surrounding Rock of the Entry for Different Seam Spacing. It is one of the purposes of rock bolting to control the deformation of surrounding rock. Figure 11 shows the deformation of the surrounding rock of the entry for different seam spacing.

As shown in Figures 11 and 12, with the increase of seam spacing, the convergence of roof-to-floor and rib-to-rib gradually decreases. In addition, the convergence of the right rib is greater than the left rib.

(1) At 5 m seam spacing, the convergence of roof-to-floor and rib-to-rib is 801 mm and 1261 mm,

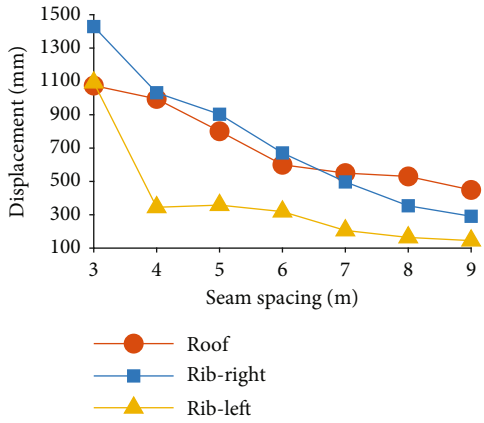

FIGURE 12: Simulation displacement of surrounding rock of the entry for different seam spacing.

respectively. The surrounding rock deformation of the entry is quite large, indicating that the rock bolting performance is terrible.

(2) When the seam spacing is no less than 6 m, the convergence of roof-to-floor and rib-to-rib is relatively small. At 6 m seam spacing, the convergence of roof-to-floor and rib-to-rib is 600 mm and 990 mm, respectively. At 9 m seam spacing, the convergence of roof-to-floor and rib-to-rib is 449 mm and 436 mm, respectively. Compared with the seam spacing of 3-5 m, the surrounding rock of the entry is well controlled.

Consequently, when the seam spacing is no less than 6 m, the rock deformation of the entry is relatively small, the yield zone around the entry is under control, and the rock bolting performance is relatively good.

6. Discussion

In Section 3, through theoretical analysis, it was found that the peak value of front abutment pressure is 2.5 m in front of the panel, and then the floor failure depth of the No.3-1 coal seam (UCS) was 3.2 m. Compared to the previous calculation results, the value of L is minor, mainly because the buried depth H of the No.3-1 coal seam (UCS) is small, and L is closely related to H (see Equation (2)).

The result of the pull-out test of roof bolting in Section 4 showed that the pull-out force of bolt can reach 30kN at the seam spacing of more than 6 m, suggesting that the rock bolts can be anchored in the relatively intact rock strata, which was consistent with the suspension theory.

Section 5 determined that the maximum failure depth of the No.3-1 coal seam (UCS) is 3.0-3.3 m by numerical simulation, which was consistent with the theoretical analysis results in Section 3. Furthermore, the simulation results showed that the rock bolting performance is good when the seam spacing exceeds 6 m, which coincided with the pull-out test in Section 4.

What is noteworthy is that this work was based on Chaili Coal Mine. Due to different mining and geological conditions, the applicability of presented theoretical analysis, pull-out test, and numerical simulation methods on other coal mines should be further studied.

7. Conclusions

(1) The maximum floor failure depth calculated by the theoretical analysis was 3.2 m. Generally, the anchorage length of the rock bolt is less than 2.4 m. Thus, the roof bolting seam spacing is at least 5.6 m.

(2) The pull-out bolt test was carried out on the lower coal seam's entry roof. The results show that when the seam spacing is no less than 6 m, the drawing force is more significant than 30kN. Therefore, the minimum seam spacing of roof bolting is taken as 6 m.

(3) Numerical simulation was set out to seek the floor failure depth and the performance of roof bolting. Simulation results show that the floor failure depth of the upper coal seam is 3.0-3.3 m. Compared with 3-5 m seam spacing, when the seam spacing is no less than 6 m, the yield zone of the lower coal seam's roof is relatively not large. The surrounding rock deformation of the entry significantly decreases, indicating that the performance of roof bolting is good.

In conclusion, through theoretical analysis, pull-out bolt test, and numerical simulation, this paper determines the minimum seam spacing of roof bolting is 6 m, where the entry under the gob of the close-distance coal seam. This study quantitatively studies the influence of seam spacing on selecting support methods, providing a reference for roof bolting design of coal entry under similar conditions.

Data Availability

The data used to support the findings of this study are available from the corresponding author upon request.

Conflicts of Interest

The authors declare that they have no conflicts of interest.

Acknowledgments

This research was funded by the National Natural Science Foundation of China (Grant nos. 51574156 and 52074166).

References

[1] S. Jie, L. Zhen-hua, H. Cun-han, C. Zheng-zheng, X. You-lin, and C. Zu-guo, "Catastrophe mechanism of stress-fissure coupling field in mining close distance seams in Southwest China," *Geofluids*, vol. 2021, 9 pages, 2021.

[2] Y. Li, Y. Ren, S. Peng, H. Cheng, N. Wang, and J. Luo, "Measurement of overburden failure zones in close-multiple coal

seams mining," *International Journal of Mining Science and Technology*, vol. 31, no. 1, pp. 43–50, 2021.

[3] Y. Li, J. Wang, Y. Chen, Z. Wang, and J. Wang, "Overlying strata movement with ground penetrating radar detection in close-multiple coal seams mining," *International Journal of Distributed Sensor Networks*, vol. 15, no. 8, 2019.

[4] X. Li, W. He, and Z. Xu, "Study on law of overlying strata breakage and migration in downward mining of extremely close coal seams by physical similarity simulation," *Advances in Civil Engineering*, vol. 2020, 11 pages, 2020.

[5] F. Cui, C. Jia, X. Lai, Y. Yang, and S. Dong, "Study on the law of fracture evolution under repeated mining of close-distance coal seams," *Energies*, vol. 13, no. 22, p. 6064, 2020.

[6] F. Cui, C. Jia, and X. Lai, "Study on deformation and energy release characteristics of overlying strata under different mining sequence in close coal seam group based on similar material simulation," *Energies*, vol. 12, no. 23, p. 4485, 2019.

[7] J. Ning, J. Wang, Y. Tan, and Q. Xu, "Mechanical mechanism of overlying strata breaking and development of fractured zone during close-distance coal seam group mining," *International Journal of Mining Science and Technology*, vol. 30, no. 2, pp. 207–215, 2020.

[8] J. Zhang and B. Wang, "Study on the bearing structure and stability of overlying strata: an interval gob in shallow buried coal mining of Northwest China," *Arabian Journal of Geosciences*, vol. 14, no. 4, 2021.

[9] W. Zhang, D. Zhang, D. Qi, W. Hu, Z. He, and W. Zhang, "Floor failure depth of upper coal seam during close coal seams mining and its novel detection method," *Energy Exploration & Exploitation*, vol. 36, no. 5, pp. 1265–1278, 2018.

[10] Z. Sun, Y. Wu, Z. Lu, Y. Feng, X. Chu, and K. Yi, "Stability analysis and derived control measures for rock surrounding a roadway in a lower coal seam under concentrated stress of a coal pillar," *Shock and Vibration*, vol. 2020, 12 pages, 2020.

[11] Y. Tan, T. Zhao, and Y. Xiao, "In situ investigations of failure zone of floor strata in mining close distance coal seams," *International Journal of Rock Mechanics and Mining Sciences*, vol. 47, no. 5, pp. 865–870, 2010.

[12] X. Liu, X. Li, and W. Pan, "Analysis on the floor stress distribution and roadway position in the close distance coal seams," *Arabian Journal of Geosciences*, vol. 9, no. 2, 2016.

[13] X. Wang, J. Wang, X. Chen, and Z. Chen, "A roadway in close distance to coal seam in deep mine: location selection and supporting practice based on creep characteristics of surrounding rocks," *Archives of Mining Sciences*, vol. 66, no. 3, pp. 407–419, 2021.

[14] G. Wu, X. Fang, H. Bai, M. Liang, and X. Hu, "Optimization of roadway layout in ultra-close coal seams: a case study," *PLoS One*, vol. 13, no. 11, article e0207447, 2018.

[15] X. Gao, S. Zhang, Y. Zi, and S. K. Pathan, "Study on optimum layout of roadway in close coal seam," *Arabian Journal of Geosciences*, vol. 13, no. 15, 2020.

[16] Y. Zhang, J. Yang, J. Zhang et al., "Modeling the spatial and temporal evolution of stress during multiworking face mining in close distance coal seams," *Advances in Civil Engineering*, vol. 2021, Article ID 5624972, 11 pages, 2021.

[17] W. Zhang, J. Guo, K. Xie et al., "Comprehensive technical support for safe mining in ultra-close coal seams: a case study," *Energy Exploration & Exploitation*, vol. 39, no. 4, pp. 1195–1214, 2021.

[18] Z. Zhang, M. Deng, J. Bai, S. Yan, and X. Yu, "Stability control of gob-side entry retained under the gob with close distance coal seams," *International Journal of Mining Science and Technology*, vol. 31, no. 2, pp. 321–332, 2021.

[19] W. Sun, Z. Qin, Q. Li, G. Chen, and T. Li, "Study on optimization of roadway position in pre-mining upper layered concave–convex coal body," *Geotechnical and Geological Engineering*, vol. 37, no. 5, pp. 3739–3748, 2019.

[20] Z M G o S Energy, *Technical Specifications for Rock Bolting in Coal Mine Roadways in Zibo Mining Group*, China Coal Industry Publishing House, Beijing, 2013.

[21] Technical specifications for rock bolting in coal mine roadways, GB/T 35056-2018. (2018).

[22] Z. Guangchao, Z. Chuanwei, C. Miao et al., "Ground response of entries driven adjacent to a retreating longwall panel," *International Journal of Rock Mechanics and Mining Sciences*, vol. 138, p. 104630, 2021.

[23] G. Zhang, Z. Wen, S. Liang et al., "Ground response of a gob-side entry in a longwall panel extracting 17 m-thick coal seam: a case study," *Rock Mechanics and Rock Engineering*, vol. 53, no. 2, p. 497, 2020.

[24] G. Zhang, F. He, H. Jia, and Y. H. Lai, "Analysis of gateroad stability in relation to yield pillar size: a case study," *Rock Mechanics and Rock Engineering*, vol. 50, no. 5, pp. 1263–1278, 2017.

[25] G. Zhang, Y. Li, X. Meng et al., "Distribution law of in situ stress and its engineering application in rock burst control in Juye mining area," *Energies*, vol. 15, no. 4, p. 1267, 2022.

[26] G. Zhu, B. Liu, L. Dou, Y. P. Wu, and Z. W. Ding, "Numerical simulation for whole process of longwall mining on the basis of goaf compaction effect," *Journal of China University of Mining and Technology*, vol. 48, no. 4, pp. 775–783, 2019.

[27] Q. Bai, S. Tu, Y. Yuan, and F. T. Wang, "Back analysis of mining induced responses on the basis of goaf compaction theory," *Journal of China University of Mining and Technology*, vol. 42, no. 3, p. 355, 2013.